ScientificScholar®
Knowledge is power
Publisher of Scientific Journals

American Journal of Pharmacotherapy and Pharmaceutical Sciences

Original Research Article *Pharmaceutical Technology and Manufacturing*

Characterization of physicochemical properties of microcrystalline and nanocrystalline cellulose powders derived from *Citrullus lanatus* peels for potential pharmaceutical applications

Chukwuemeka Paul Azubuike, PhD[1], Adepeju Racheal Adedokun[1], Bukola Aminat Oseni[1], Modupe Ologunagba[1], Shadrack Joel Madu[2]

[1]Department of Pharmaceutics and Pharmaceutical Technology, Faculty of Pharmacy, University of Lagos, Lagos, Nigeria.
[2]School of Pharmacy, De Montfort University, Leicester, United Kingdom.

***Corresponding author:**
Chukwuemeka Paul Azubuike, PhD
Department of Pharmaceutics and Pharmaceutical Technology, Faculty of Pharmacy, University of Lagos, Lagos, Nigeria.

cazubuike@unilag.edu.ng

Received: 07 April 2024
Accepted: 14 August 2024
Published: 17 January 2025

https://ajpps.org

DOI
10.25259/AJPPS_2025_002

Quick Response Code:

ABSTRACT

Objectives: Agricultural residues represent a potential source of cellulose. *Citrullus lanatus* (watermelon) peel, an agricultural waste, was investigated as a potential sustainable source for the production of low-cost pharmaceutical-grade cellulose-based materials.

Materials and Methods: The physicochemical properties of the cellulose-based samples (microcrystalline and nanocrystalline celluloses) obtained from watermelon peel were investigated through physicochemical tests including Fourier-transform infrared spectroscopy, powder X-ray diffraction, differential scanning calorimetry, thermogravimetric analysis, laser diffraction, and dynamic image analysis. The effects of acid hydrolysis and drying methods on the particle size and particle size distribution (PSD) of the celluloses were evaluated.

Results: The particle size analysis revealed that particle sizes became smaller, and the PSD narrowed with acid hydrolysis treatment. The spread of the particle sizes of the watermelon peel microcrystalline cellulose in terms of width and length was similar to watermelon peel native cellulose having width <170 µm and length <200 µm while the particles of the watermelon peel nanocrystalline cellulose (oven dried) had width <80 µm and length <100 µm. The spectroscopic analysis revealed that the extracted cellulose samples consisted of crystalline cellulose I and cellulose II polymorphs, and the degree of crystallinity increased after acid hydrolysis treatment. The thermal analysis revealed that the cellulose samples followed a similar degradation pattern. Freeze-dried nanocrystalline cellulose exhibited high thermal stability. The nanocellulose samples had similar swelling capacities.

Conclusion: The microcrystalline and nanocrystalline cellulose obtained from watermelon peel possessed improved physicochemical properties and can be explored as low-cost excipients in manufacturing pharmaceutical dosage forms.

Keywords: *Citrullus lanatus* peel, Microcrystalline cellulose, Nanocrystalline cellulose, Acid Hydrolysis

INTRODUCTION

Cellulose is a polysaccharide that is abundant in nature and is an essential structural component in the cell walls of plants.[1] Cellulose is a straight-chain polymer made up of repeating units of

D-glucose monomers joined by β (1→4)-glycosidic bonds.[2] Cellulose is an important excipient used in the manufacture of solid dosage formulations to influence performance during drug manufacture, the performance of final drug products, and the quality control of the drug product.

Cellulose is primarily sourced from wood, cotton, flax, hemp, and jute plants for industrial purposes. However, a considerable volume of cellulose-containing resources ends up as waste following their utilization and or production processes, such as in agricultural residues such as sugarcane bagasse, fruit peels, fallen branches, leaves, twigs, sawdust, grass stalks, and husks.[3] These wastes have gained tremendous interest due to their availability, high volume, and the low cost of obtaining them.[3] Fruit peels are a source of cellulose, and their utilization in the production of cellulose for various applications could help eliminate their contribution to environmental pollution.

Citrullus lanatus (watermelon) is an edible tropical fruit that belongs to the *Cucurbitaceae* family. It is native to tropical areas of Africa, although it is cultivated worldwide, with about 166 million tons being produced annually.[4] Watermelon peel, which constitutes 30% w/w of the total fruit, is generated as waste from use in restaurants, small-scale fruit juice production by fruit vendors, and food beverage processing lines; this results in the generation of a considerable volume of organic waste.[5] The structural composition of watermelon fruit peels includes cellulose, hemicellulose, lignin, pectin, and a small number of extractives.[6] Cellulose is isolated from other components by combining chemical, enzymatic, or mechanical treatments.[7] The chemical method involving the alkaline treatment of biomass is the most widely used because it offers the advantages of low temperature and pressure requirements and higher efficiency in the breakdown and solubilization of the lignin and hemicellulose from the biomass.[8]

Microcrystalline and nanocrystalline cellulose are derived from cellulose by subjecting cellulose microfibrils to mechanical and chemical treatments which isolate its highly ordered crystalline regions and eliminate the amorphous regions.[2] This crystalline cellulose possesses remarkable characteristics such as biodegradability, a high aspect ratio, large specific surface area, high specific strength, highly reactive surface groups, and low density.[2] Microcrystalline cellulose (MCC) is widely used in pharmaceuticals as binders, diluents, disintegrants, and extrusion-spheronization processes in tablet and capsule formulations.[9] On the other hand, nanocrystalline cellulose is being explored for utilization as carriers in drug delivery systems such as nanoparticles, microparticles, hydrogels, and nanogel, as a vehicle to control the release of incorporated drugs in transdermal preparations to improve efficacy and in tissue bioscaffold for cellular growth, tissue repair, and regeneration.[10]

The commercial sources of cellulose for pharmaceutical applications are mainly woods and plants; continuous depletion of these resources leads to its scarcity as well as has a negative impact on the natural ecosystems and climate. Therefore, there is a need to explore alternative sources of cellulose. Agricultural wastes from plants such as the watermelon peel represent an alternative source of cellulose. This research is aimed at generating low-cost microcrystalline and nanocrystalline cellulose from the native cellulose extracted from watermelon peel and evaluating their physicochemical properties for potential pharmaceutical applications to provide an alternatively cheaper source of cellulose and convert waste to wealth.

MATERIALS AND METHODS

Materials

The watermelon peel, which consists of the rind and outer flesh, was obtained from vendors at the Mushin market, Mushin, Lagos State, Nigeria. The analytical grade of sodium hydroxide (97%), hydrochloric acid (36%), sulfuric acid (98%), and sodium hypochlorite solution (4%w/v) was purchased from central drug house (CDH) Fine Chemicals (India).

Extraction of cellulose from watermelon peel

The watermelon peel was washed, cut, and sun-dried for three days. It was, further, dried in the oven at 80°C for 90 min, ground, and passed through a sieve of 1.204 mm aperture size to obtain the watermelon peel powder. A stepwise extraction process based on Akter *et al.* 2015[11] was adopted with some modifications. Watermelon peel powder of 500 g was weighed and boiled in water at 100°C for 1 h. The mixture was filtered, and the solid mass was thoroughly washed with water. The residue was immersed in 5 L of 17.5% w/v sodium hydroxide solution and heated at 100°C for 5 h with intermittent stirring every 15 min to solubilize the lignin, hemicellulose fraction, and other extractives. The reaction mixture was filtered, and the solid mass was washed with water until the water was neutral when tested with red litmus paper. The residue was bleached with 3.2% w/v sodium hypochlorite solution at 40°C for 40 min. The reaction mixture was filtered and washed thoroughly with water until it was neutral to red litmus paper. The treatment of the residue with sodium hydroxide followed by sodium hypochlorite solutions was repeated, washing thoroughly with water after each treatment to obtain the native cellulose (α-cellulose). The yield of the native cellulose was calculated using Equation 1.

$$\% \text{ Yield} = \frac{\text{Weight of native cellulose}}{\text{Weight of watermelon peel powder}} \times 100$$

(Equation 1)

Synthesis of watermelon peel microcrystalline and nanocrystalline cellulose

The isolated cellulose was hydrolyzed by heating with 2 M HCl at 100°C for 1 h. The ratio of acid to cellulose was kept constant at 20:1. The reaction mixture was filtered, and the residue was washed with water until it was neutral to blue litmus paper to obtain the MCC.[12] The MCC obtained was air-dried for 24 h and the yield was calculated using Equation 2.

$$\% \text{ Yield} = \frac{\text{Weight of microcrystalline cellulose produced}}{\text{Weight of native cellulose}} \times 100 \qquad \text{(Equation 2)}$$

Nanocrystalline cellulose was obtained from the native cellulose by adopting the method of Sainorudin *et al.* 2022[13] with some modifications. Native cellulose was weighed and dispersed in 64% w/v sulfuric acid solution at a cellulose to solvent ratio of 1:20 at 25°C for 60 min with constant stirring. Water was added to the mixture at a water:mixture ratio of 100:1. The suspension obtained was centrifuged for 15 min at 10,000 rpm and the supernatant was discarded. The residue was washed with water and centrifuged after each washing for 15 min at 10,000 rpm (five cycles) to remove the excess sulfuric acid indicated by no color change to blue litmus paper. The suspension was immersed in 3.2% w/v sodium hypochlorite at 25°C at a suspension-to-sodium hypochlorite solution volume ratio of 4:1, stirred once, and allowed to stand for 10 min to attain a white color. An equal volume of water was added to the mixture, and the supernatant was decanted. This mixture was washed with water three times to obtain nanocrystalline cellulose.

The nanocrystalline cellulose suspension obtained was either subjected to freeze drying ($NCC_{freeze\ dried}$) or dried in an oven at 70°C for 40 min. The oven-dried nanocellulose sheets were blended into powder ($NCC_{oven\ dried}$) and the yield was calculated using Equation 3.

$$\% \text{ Yield} = \frac{\text{Weight of nanocrystalline cellulose produced}}{\text{Weight of native cellulose}} \times 100 \qquad \text{(Equation 3)}$$

Characterization of watermelon celluloses

pH

The pH of 2 g of each cellulose sample dispersed in 100 mL of distilled water was determined using a pH meter.[14]

Solubility in water

One gram of each cellulose powder was placed in a test tube containing 20 mL of distilled water. The test tube was shaken vigorously for 10 min and observed for solubility.[15]

Moisture content

Five grams of each powder was placed in a pre-weighed porcelain dish. The dish containing the sample was placed in the oven at 105°C until a constant sample weight was obtained.[16] After cooling, the dish containing the powder was reweighed and the sample's moisture content was calculated from Equation 4.

$$\text{Moisture content } (\%) = \frac{W_2 - W_3}{W_2 - W_1} \times 100 \qquad \text{(Equation 4)}$$

Where W1 – weight of porcelain dish; W2 – weight of porcelain dish and sample before drying; and W3 – weight of porcelain dish and sample after drying.

Micromeritics

The bulk and tapped Density, Carr's compressibility index, Hausner's ratio, and angle of repose of each cellulose sample were determined according to the methods of Azubuike *et al*. 2018.[17]

Water holding capacity (WHC) and swelling capacity

The cellulose samples' water holding and swelling capacity were determined by the methods of Azubuike *et al.* 2018 and Oluwasina *et al.* 2017, respectively.[17,18]

Ash content

Two grams of the sample were weighed into a crucible and placed in the furnace. The sample was ignited at 400°C for 30 min and 800°C for 45 min.[19] The percentage of ash was calculated using Equation 5.

$$\% \text{ Ash} = \frac{\text{Weight of ash}}{\text{Weight of cellulose sample}} \qquad \text{(Equation 5)}$$

Particle size analysis

The particle size, size distribution, and morphological analysis of the test samples were determined using a SYNC analyzer (MICROTRAC Retsch GmbH, Hann, Germany). The operating conditions were set at a runtime of 40 s and a dispersion pressure of 0.5 psi. The particle size distributions (PSD) (D10, D50, D90, and mean particle size) of the solid particles were compared.[20] The data were analyzed by the Microtrac® FLEX software (12.0.0.1).

Fourier-transform infrared (FT-IR) spectroscopy

For the FTIR analysis of the cellulose samples, the spectra were collected using an ALPHA II spectrometer (Bruker UK Limited, Coventry, UK) equipped with a horizontal universal

attenuated total reflectance accessory. An average of 30 scans was collected per spectrum with a resolution of 2 cm^{-1} in the spectral region of 400–4000 cm^{-1} using the OPUS software at room temperature.[20]

Powder X-ray diffraction (PXRD)

The crystallinity of each cellulose sample was determined using the X-ray diffractometer at 25°C. Powder X-ray diffraction patterns of solids were recorded in the range of 2–40° (2θ) at a scanning rate of 0.4° (2θ) min^{-1} by a D2 PHASER diffractometer equipped with an LYNXEYE XE-T detector (Bruker UK Limited, Coventry, UK).[20] Cu–Kα radiation was used with a voltage of 30 kV and a current of 10 mA.

Thermal properties determination

Differential scanning calorimetry (DSC) analysis was carried out using a DSC 214 Polyma differential scanning calorimeter (NETZSCH instrument, Wolverhampton, UK) operated under a nitrogen atmosphere. Approximately 6 mg of the cellulose samples were placed in an aluminium pan and sealed. Measurements were conducted at a heating rate of 20˚C/min from 25°C to 400°C.[20] For the thermogravimetric analysis (TGA), the decomposition of cellulose samples was measured by a TG 209 F3 Tarsus thermogravimeter (NETZSCH Instrument, Wolverhampton, UK) operated under a nitrogen atmosphere. A five-milligram sample was analyzed in a pan with no lid. Measurements were carried out at a heating rate of 20°C min^{-1} with a temperature range 20–700°C.[20]

Statistical analysis

The measurements of the test parameters of the cellulose samples were carried out in triplicate and expressed as mean ± standard deviation. The sample means were compared using a one-way analysis of variance on Jamovi® Software. Significant differences ($P < 0.05$) were determined by the Tukey *post hoc* test using the same software.

RESULTS

Yield

The percentage yield of native cellulose obtained from watermelon peel was 18.1%, while the yield of watermelon peel MCC (Wmp-MCC), watermelon peel nanocrystalline cellulose (Wmp-$NCC_{oven\ dried}$ and Wmp-$NCC_{freeze\ dried}$) from native cellulose was 56.45% and 51.03%, respectively.

Physicochemical characterization

The physicochemical properties of the cellulose samples are presented in Table 1. All samples were insoluble in water. The pH and moisture content of the cellulose samples ranged from 6.10–7.40 to 3.90–5.87, respectively. The bulk density, tapped density, Hausner's ratio, and Carr's index of microcrystalline and oven-dried nanocrystalline cellulose were similar but significantly different than that of the native and freeze-dried nanocrystalline cellulose. All samples had a similar angle of repose. Microcrystalline and nanocrystalline cellulose held a lesser amount of water than the native cellulose. However, the micro and nanocrystalline cellulose swell more than the native cellulose, with the highest swelling capacity observed in the nanocrystalline cellulose sample.

Particle size and percentile distribution analysis

The particle size and percentile distribution of the cellulose samples are shown in Tables 2 and 3. There was a decrease in the particle size of microcrystalline and nanocrystalline cellulose when compared with the native cellulose; the nanocrystalline cellulose samples had a mean area diameter of <100 μm.

Structural characterization

The structures of the cellulose samples were analyzed by FTIR spectroscopy and powder X-ray diffraction. The FTIR spectra and X-ray diffractograms are presented in Figures 1 and 2, respectively. The degree of crystallinity of the cellulose samples derived rom the X-ray diffractogram is shown in Table 4. An increase in crystallinity was observed in the microcrystalline and nanocrystalline cellulose when compared with the native cellulose.

Thermal analysis

The thermal properties of the cellulose samples were determined by DSC and TGA analysis. The DSC and TGA thermograms are shown in Figures 3 and 4, respectively. The weight loss and its temperature derived from the TGA are presented in Table 5.

DISCUSSION

Physicochemical characterization

The pH of all cellulose samples falls within the acceptable limits of 5.0–7.5 according to the specifications in the British Pharmacopoeia 2021.[21] All cellulose samples were insoluble in water; the nanocrystalline cellulose dispersed in water to form a milky suspension that settled with time. The ability to redisperse in a medium is a highly desired characteristic in nanocrystalline cellulose products, influencing its potential applicability.[22]

The moisture content of pharmaceutical material affects its stability on storage and agglomeration properties, ultimately

Table 1: Physicochemical properties of the native modified cellulose.

Physicochemical properties	Wmp-Native	Wmp-MCC	Wmp-NCC$_{ovendried}$	Wmp-NCC$_{freeze\ dried}$
Solubility in water	Insoluble	Insoluble	Insoluble	Insoluble
pH	7.40±0.17	6.67±0.15	6.23±0.08	6.10±0.22
Moisture content	5.77±0.25	4.53±0.31	3.90±0.36	5.87±0.21
Bulk density (g/mL)	0.39±0.01	0.72±0.02	0.74±0.03	0.32±0.00
Tapped density (g/mL)	0.58±0.02	0.98±0.03	0.97±0.03	0.50±0.00
Hausner ratio	1.49±0.02	1.37±0.03	1.31±0.08	1.56±0.01
Carr's index	32.94±0.96	26.81±1.39	23.28±4.67	36.13±0.50
The angle of Repose (°)	31.36±0.89	32.69±1.05	31.71±1.02	32.83±2.78
Water holding capacity	3.05±0.38	1.20±0.10	1.55±0.28	2.53±0.09
% Swelling capacity	46.7±3.3	60.7±1.8	106.0±11.6	103.5±3.5
Swelling ratio	1.46±0.04	1.61±0.02	2.06±0.12	2.03±0.03
% Ash content	0.038±0.010	0.056±0.020	0.113±0.031	0.124±0.005

Wmp-Native: Watermelon peel native cellulose, Wmp-MCC: Watermelon peel microcrystalline cellulose, Wmp-NCC$_{oven\ dried}$: Watermelon peel nanocrystalline (oven dried), Wmp-NCC$_{freeze\ dried}$: Watermelon peel nanocrystalline cellulose (freeze-dried)

Table 2: Particle size measurement of the cellulose samples.

Parameter	Wmp-Native	Wmp-MCC	Wmp-NCC$_{oven\ dried}$	Wmp-NCC$_{freeze\ dried}$
Mean volume diameter (µm)	229.70	196.70	143.40	87.61
Mean area diameter (µm)	149.80	111.80	95.96	46.27
Specific surface area (M^2/cc)	0.04	0.054	0.063	0.13
SD	130.00	129.40	76.07	63.75
Graphic mean (Mz)	229.30	195.00	140.70	86.37
Graphic skewness (Ski)	0.0387	0.0794	−0.0552	0.2846
Graphic kurtosis (Kg)	0.7960	0.0758	0.8510	0.7790

Wmp-Native: Watermelon peel native cellulose, Wmp-MCC: Watermelon peel microcrystalline cellulose, Wmp-NCC$_{oven\ dried}$: Watermelon peel nanocrystalline (oven dried), Wmp-NCC$_{freeze\ dried}$: Watermelon peel nanocrystalline cellulose (freeze-dried), SD: Standard deviation

Table 3: Percentile distribution of particle sizes D10, D50, and D95.

Percentiles	Wmp-Native (µm)	Wmp-MCC (µm)	Wmp-NCC$_{oven\ dried}$ (µm)	Wmp-NCC$_{freeze\ dried}$ (µm)
D10	757.60	512.50	474.80	21.47
D50	226.70	190.60	146.40	75.67
D95	417.50	383.20	259.30	192.4
Mean (µm)	229.70	196.70	143.40	87.61

Wmp-NCC$_{oven\ dried}$: Watermelon peel nanocrystalline (oven dried), Wmp-NCC$_{freeze\ dried}$: Watermelon peel nanocrystalline cellulose (freeze-dried)

affecting the quality, safety, and efficacy of the finished pharmaceutical product. The moisture content of MCC fell within the acceptable limits of ≤5% (w/w) according to British Pharmacopoeia 2021 specifications for MCC; the oven-dried nanocrystalline had a moisture content of 3.90% while those of native cellulose and freeze-dried nanocrystalline cellulose were similar but higher than that of the oven-dried nanocrystalline cellulose at 5.77% and 5.87%, respectively [Table 1]. Excessive moisture content in cellulose can result in microbial instability during storage, swelling, and aggregation of the cellulose particles, which can lead to loss of flowability, compressibility, and reduced binding properties when used as an excipient in solid dosage forms; this, in turn, leads to non-uniformity and inconsistency in the content of the final tablet or capsule formulation.[23]

In this study, the microcrystalline and oven-dried nanocrystalline cellulose had comparable bulk and tapped densities, which were higher than those of native cellulose and freeze-dried nanocrystalline cellulose, which were also similar. Higher bulk and tapped density show that the powder has weaker inter-particle forces and bonds, which predispose it to less resistance in the packing and a better potential to flow and rearrange the particles during compression.[24] Therefore, microcrystalline and oven-dried nanocrystalline cellulose may have better flow properties than the native and freeze-dried nanocrystalline. Although bulk and tapped densities

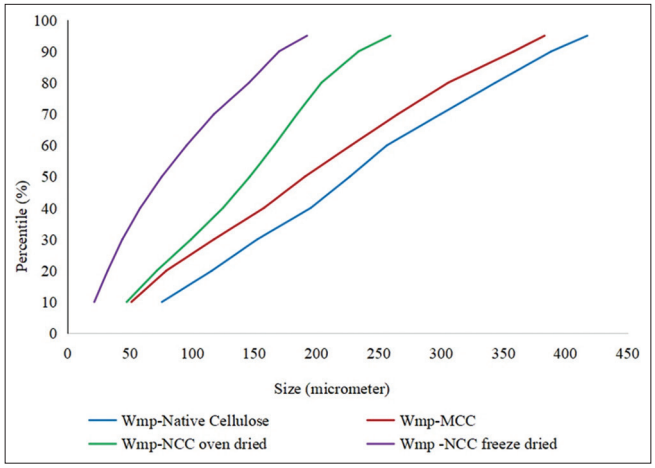

Figure 1: Percentile distribution of particle size in watermelon peel native cellulose, watermelon peel microcrystalline cellulose, watermelon peel oven-dried nanocrystalline cellulose (Wmp-$NCC_{oven\ dried}$), and watermelon peel freeze-dried nanocrystalline cellulose (d) Wmp-$NCC_{freeze\ dried}$.).

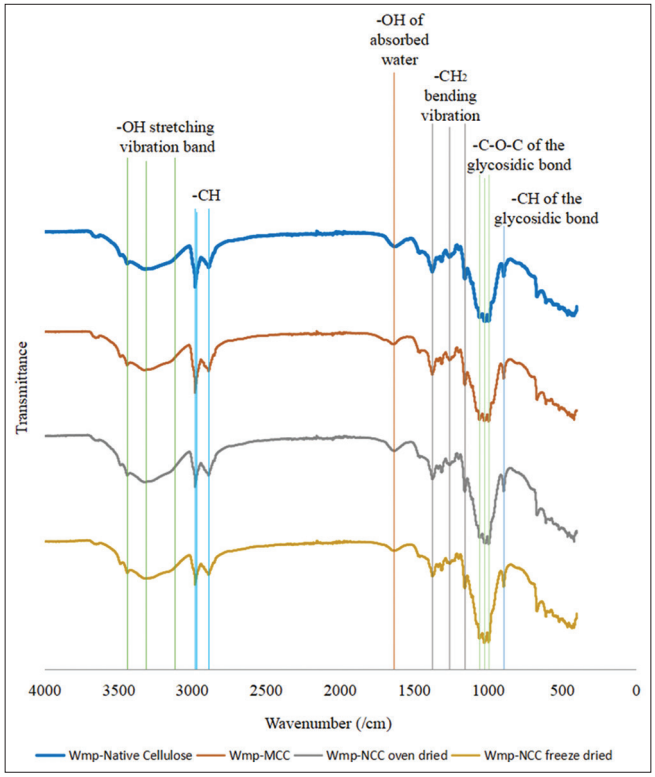

Figure 2: Fourier transform infrared spectra of watermelon peel native cellulose, watermelon peel microcrystalline cellulose, watermelon peel oven-dried nanocrystalline cellulose (Wmp-$NCC_{oven\ dried}$), and watermelon peel freeze-dried nanocrystalline cellulose (Wmp-$NCC_{freeze\ dried}$).

are not intrinsic properties of a powder due to the ability to change based on how the material is handled, they are still critical powder properties used in the making decisions such as the size of vessels to be utilized in the production process.[24]

Table 4: Crystallinity of the cellulose samples.

Sample	Degree of crystallinity (CrI) (%)
Wmp-native cellulose	65.2
Wmp-MCC	74.0
Wmp-$NCC_{oven\ dried}$	71.4
Wmp-$NCC_{freeze\ dried}$	72.4

Wmp-Native: Watermelon peel native cellulose, Wmp-MCC: Watermelon peel microcrystalline cellulose, Wmp-$NCC_{oven\ dried}$: Watermelon peel nanocrystalline (oven dried), Wmp-$NCC_{freeze\ dried}$: Watermelon peel nanocrystalline cellulose (freeze-dried)

Hausner's ratio, Carr's compressibility index, and repose angle measure powders or granules' flowability to ensure content uniformity and consistent drug levels in solid dosage formulations. Hausner's ratios of 1.12–1.18, 1.19–1.25, 1.26–1.34, 1.35–1.45, and 1.46–1.59 indicate good, fair, passable, poor, and inferior flow, respectively; Carr's indices of <10, 11–15, 16–20, 21–25, 26–31, and 32–37 indicate excellent, good, fair, passable, poor, and inferior powder flows, respectively, while the angles of repose of 25–30, 31–35 and 36–40, 41–45, and >46° indicate excellent, good, fair, passable, and poor flows, respectively. The oven-dried nanocrystalline cellulose had a better flow than the other types of cellulose with a Hausner's ratio of 1.31 and Carr's index of 23.28 [Table 1], which indicates a passable flow. The MCC (Hausner's ratio – 1.37, Carr's index – 26.81) exhibited a better flow than the native cellulose (Hausner's ratio –1.49, Carr's index –32.94) and freeze-dried nanocellulose (Hausner's ratio –1.56, Carr's index – 36.13), which showed an inferior flow. The improvement in the flow property of microcrystalline and oven-dried nanocellulose, when compared with the native cellulose, may be due to the acid hydrolysis treatment undergone by the powders because hydrolysis breaks long cellulose fibers to smaller particles having lesser contact area which results in increased flowability.[25] Although freeze-dried nanocellulose exhibited very poor flow properties despite acid hydrolysis, this may be due to the higher moisture content. The result for the angle of repose was not consistent with that of Hausner's ratio and Carr's index; there was no statistically significant difference in the angles of repose of the cellulose powders, which fell within the range of 31.36–32.83 which indicated that all cellulose powders possessed a good flow property.

WHC refers to the ability of the cellulose polymer to hold water molecules within its structure without dissolving in it. In general, cellulose tends to interact strongly with water by hydrogen bonding.[26] The native cellulose held more water molecules than the other cellulose while the microcrystalline and oven-dried nanocellulose held the least amount of water. The high-WHC shown by the native cellulose might be due to the presence of amorphous cellulose regions which are unstable when they interact with water compared to the other

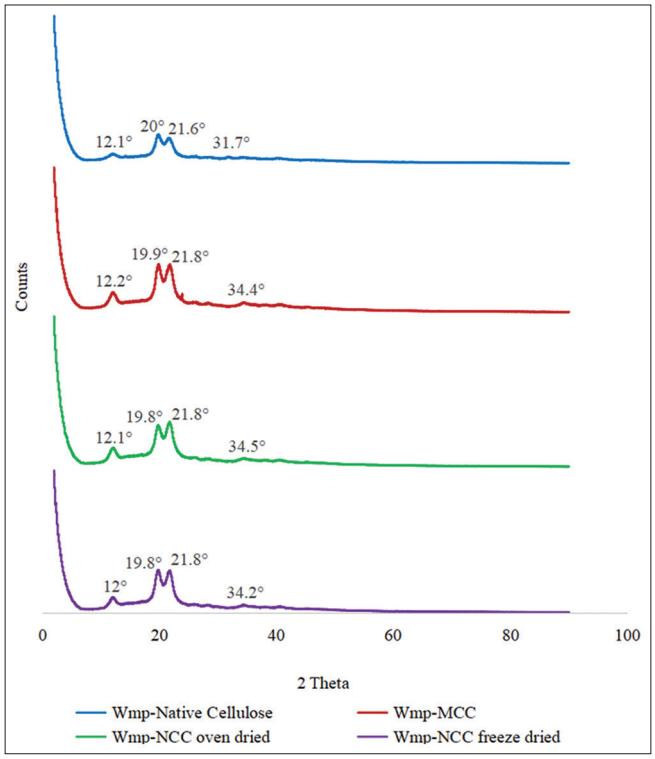

Figure 3: X-ray diffraction spectra of watermelon peel native cellulose, watermelon peel microcrystalline cellulose, watermelon peel oven-dried nanocrystalline cellulose (Wmp-$NCC_{oven\ dried}$), and watermelon peel freeze-dried nanocrystalline cellulose (Wmp-$NCC_{freeze\ dried}$).

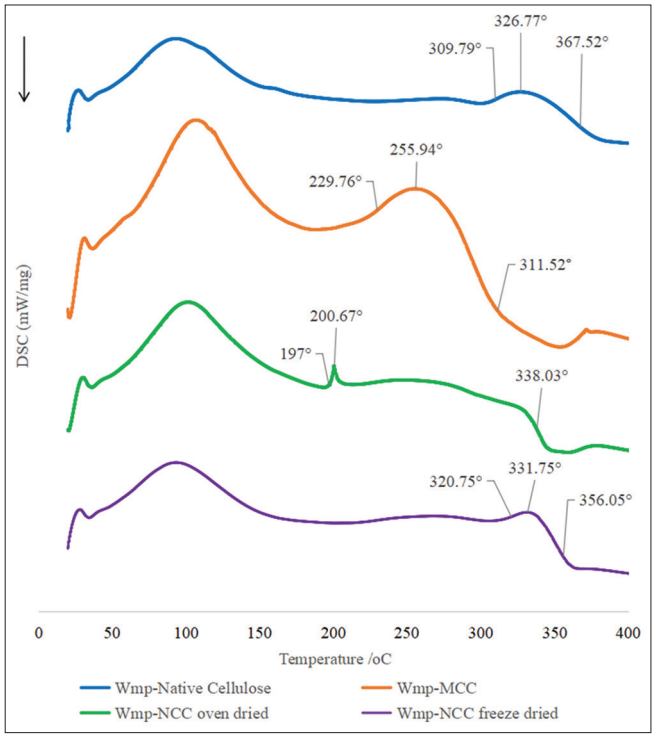

Figure 4: Differential scanning calorimetry thermogram of watermelon peel native cellulose, watermelon peel microcrystalline cellulose, watermelon peel oven-dried nanocrystalline cellulose (Wmp-$NCC_{oven\ dried}$), and watermelon peel freeze-dried nanocrystalline cellulose (Wmp-$NCC_{freeze\ dried}$).

cellulose powders in which the amorphous cellulose regions have been disrupted to isolate the crystalline cellulose by subjecting to acid hydrolysis.[27] The significant WHC shown by the freeze-dried nanocellulose powder that is comparable to native cellulose may be due to a more porous sponge-like microstructure imparted on it by the freeze-drying process; this promotes the penetration of water into the molecule leading to higher absorption kinetics and capacity. In contrast, oven drying causes shrinkage of the polymer structure while displaying a continuous matrix with a uniform surface with reduced porosity characterized by irregular pores.[28] Hence, the oven-dried nanocrystalline and MCC exhibited lower water-retaining capacity. The acid-hydrolysis-modified cellulose samples showed a higher swelling capacity than the native cellulose despite the ability of the native polymer to retain more water. The nanocrystalline cellulose had the highest swelling capacity and swelling ratios, irrespective of the drying method employed followed by the MCC.

The ash content is an important parameter used to estimate the purity and quality of cellulose samples. The ash content values of the native and MCC fell in the acceptable limits of <0.1% (w/w) according to British Pharmacopoeia 2021 specifications while those of oven-dried and freeze-dried nanocrystalline

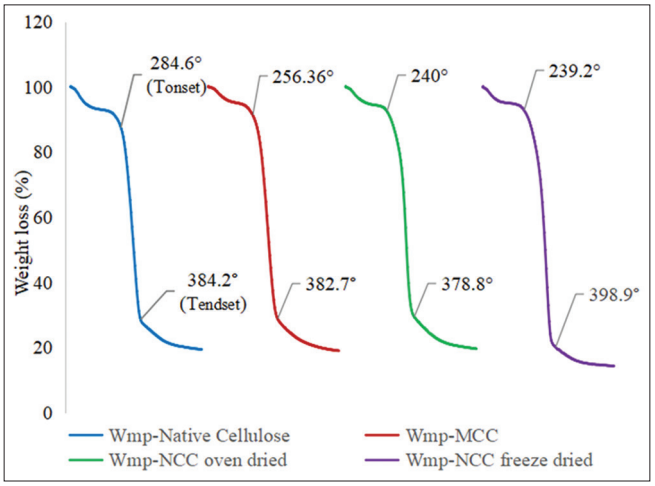

Figure 5: Thermogravimetric analysis thermogram of watermelon peel native cellulose, watermelon peel microcrystalline cellulose, watermelon peel oven-dried nanocrystalline cellulose (Wmp-$NCC_{oven\ dried}$), and watermelon peel freeze dried nanocrystalline cellulose (Wmp-$NCC_{freeze\ dried}$).

cellulose were slightly above the upper limit at 0.113% and 0.124%, respectively [Table 1].[21] The ash content may be affected by various factors such as the source of the cellulose, the processing method, and the presence of impurities.

Table 5: Thermal properties of the cellulose samples derived from thermogravimetric analysis.

Sample	Weight loss $T_{on5\%}$ (%)	$T_{on\ 5\%}$ (°C)	T_{onset} (°C)	$T_{50\%}$ (°C)	T_{Endset} (°C)	Weight loss at degradation stage (%)	Residual Weight at $T_{694.9}$°C $_{(completion)}$ (%)
Wmp-Native cellulose	6.91	100.70	284.60	349.90	384.20	73.62	19.38
Wmp-MCC	4.97	174.40	256.36	340.50	382.70	76.07	18.96
Wmp-$NCC_{oven\ dried}$	5.66	116.20	240.00	339.70	378.80	74.75	19.59
Wmp-$NCC_{freeze\ dried}$	4.85	152.70	239.20	345.90	398.90	76.70	14.30

$T_{on\ 5\%}$ (°C): Temperature at 5% weight loss, T_{onset} (°C): Temperature at the onset of decomposition, $T_{50\%}$ (°C): Temperature at 50% weight loss, T_{Endset} (°C): Temperature at the end of decomposition. Wmp-$NCC_{oven\ dried}$: Watermelon peel nanocrystalline (oven dried), Wmp-$NCC_{freeze\ dried}$: Watermelon peel nanocrystalline cellulose (freeze-dried)

Particle size analysis

A decrease in the mean volume diameter of the cellulose samples was observed on acid hydrolysis as the size of native cellulose (229.7 ± 130 µm) >MCC (196.7 ± 129.4 µm) >oven-dried nanocellulose (143.4 ± 76.07 µm) > freeze-dried nanocellulose (87.61 ± 63.75 µm) [Table 2]. This corresponds with the observed trend in the percentile distribution [Table 3], which showed that the particle sizes of the acid-hydrolyzed (microcrystalline and nanocrystalline) cellulose were smaller. Furthermore, a decrease and narrow range in PSD was observed in the nanocellulose samples [Figure 1] as shown by the progressive reduction in the degree of variability in the mean volume particle diameter depicted by the standard deviation values [Table 2] while a wide range of variability in the PSD was observed in the native cellulose and MCC [Table 3]. The specific surface area increased in the microcrystalline and nanocrystalline cellulose; this corresponds with the observed trend of decreasing particle sizes which directly predispose to higher specific surface area in the cellulose samples. The freeze-dried nanocellulose exhibited the largest specific surface area which indicates that it would have higher surface reactivity in reaction processes and increased sorption capacity.

Graphic kurtosis is a measure of the departure of a PSD peak from normality; a graphic kurtosis value of 0.67–0.9 indicates that the PSD peak is platykurtic while <0.67 signifies very platykurtic peak distribution.[29] The cellulose samples had graphic kurtosis values (0.0758–0.851) which indicated that the PSD had a wide range with high variability and there is an increased tendency to encounter particles that are significantly larger or smaller than the average particle diameter. This is evidenced by the bimodal distributions of the particle sizes for all the materials (except the freeze-dried nanocrystalline cellulose; [Table 3]).

The particle size, PSD, particle surface area, and morphology are critical material properties that can influence the performance of the material in pharmaceutical manufacturing processes. A wide range with high variability in the particle size and size distribution such as was observed in the Wmp-native cellulose and Wmp-MCC would influence flowability, mixing efficiency, uniformity, encapsulation, and compression in the manufacturing processes for solid oral dosage forms as well as drug dissolution, bioavailability, content uniformity, and stability amongst others. Therefore, the impact of particle sizes of pharmaceutical powders on drug product manufacturability and performance should be evaluated during pre-formulation studies to establish appropriate particle size specifications to enhance the control of drug product quality and ensure manufacturing consistency.[30,31]

FTIR spectrophotometry

The FTIR spectra of the cellulose samples showed a broad absorption band in the range of 3600–3200cm^{-1} [Figure 2], which is characteristic of O-H stretching, but the spectra showed a slight decrease in the transmittance for Wmp-$NCC_{oven\ dried}$ and Wmp-$NCC_{freeze\ dried}$ than that of Wmp-native cellulose and Wmp-MCC. This may be due to an increase in the number of –OH groups on the crystalline cellulose chain following acid hydrolysis. The sharp peaks observed in the spectra at 2981cm^{-1} are characteristic stretching vibrations of –CH in the cellulose molecule which decreased in sharpness for Wmp-$NCC_{oven\ dried}$ and Wmp-$NCC_{freeze\ dried}$ due to changes in degree of crystallinity, molecular orientation, and degree of order of cellulose.[32] The characteristic peak in the spectra at 1636 cm^{-1} is the bending vibration of -OH groups due to water bound to the cellulose structure which showed an increase in the transmittance in the order – Wmp-native cellulose <Wmp-MCC <Wmp-$NCC_{oven\ dried}$ <Wmp- $NCC_{freeze\ dried}$. This indicates that the concentration of these atoms and bonds was reduced with acid hydrolysis treatment, which dissolved the amorphous cellulose region on the chain to leave behind the crystalline cellulose region. The spectra peak at 1462 cm^{-1} and 894.05–893.90 cm^{-1} represent the bending or scissoring vibration of the $–CH_2$ group and – CH deformation vibration of the glycosidic linkage bond, respectively. These two peaks are collectively referred to as the crystallinity band and are associated with the crystalline region of cellulose. The cellulose samples showed the characteristic peaks of CH and CH_2 bending at the frequency band of 1375.86–1156.74 cm^{-1} associated with amorphous

regions of cellulose in which an increase in transmittance was observed in the modified cellulose samples. This indicates a reduction of the amorphous cellulose region and increased crystallinity of the cellulose with acid hydrolysis treatment.[33] The band at 1057.28–994.62 cm^{-1} on the spectra is indicative of stretching vibrations of C-O-C glycosidic bond and ring stretching, which showed a trend of decrease in transmittance, which indicates increased crystallinity of the cellulose with acid hydrolysis treatment which causes the cellulose chains to become more ordered and tightly packed.

Powder X-ray diffraction (PXRD)

All the diffraction patterns in Figure 3 appear the same, except for their intensities, which show differences in crystallinity. The diffraction pattern of the cellulose samples in Figure 3 showed the appearance of a doublet peak at the (002) crystalline plane, which indicates the presence of cellulose crystal polymorphs; cellulose I and cellulose II. The doublet peak also appeared on the diffractogram of Wmp-native cellulose indicating that some level of partial conversion must have occurred during the sodium hydroxide pretreatment step.[34]

The various methods adopted did not appear to have affected the crystal packing of all the cellulose samples but had changed the particle sizes. Cellulose II typically exhibits diffraction peaks at about 12°, 20°, and 22°, which corresponded with the observed PXRD pattern, although small diffraction peaks were observed in the diffractogram at about 34°, with them all signifying the 101, 10Î, 002, and 004 crystallographic reflection plane, respectively.[35,36] Cellulose II exhibits increased thermal stability, tensile strength, and reduced tendency to absorb moisture, which imparts it less susceptibility to the effects of humidity; it possesses excellent binding and disintegration properties in tablet formulation over cellulose I.[34]

The diffraction peak of native cellulose became sharper with acid hydrolysis indicating an increase in crystallinity which was also reflected in the crystallinity index presented in Table 4, although the nanocellulose sample showed a slightly lower crystallinity relative to Wmp-MCC. This may be due to the effect of sulfuric acid on the crystal lattice of the cellulose as the initial alkaline pretreatment disrupts the amorphous cellulose region leaving behind the crystalline cellulose, which under harsh reaction conditions may be susceptible to further digestion. The observed increase in crystallinity is expected to impart increased strength and rigidity in cellulose which increases their potential applications.[37,38]

DSC

The DSC thermogram [Figure 4] of the cellulose samples showed the decomposition process of cellulose samples. Wmp-native cellulose and Wmp-MCC exhibited broader melting peaks while that of Wmp-$NCC_{freeze\ dried}$ was sharper but unlike Wmp-$NCC_{oven\ dried}$. Only Wmp-$NCC_{oven\ dried}$ exhibited a very sharp and small decomposition peak which indicates that a fast rate of transformation occurred with large enthalpy changes. Crystalline regions in polymers have ordered structures that cause restriction of molecular mobility but in the nanocellulose samples which also showed a high degree of crystallinity, their thermogram exhibited sharper peaks due to the presence of a more uniform crystalline structure such that disturbance at one crystal lattice results in disruption in all other structurally associated lattices.[39]

Wmp-native cellulose and Wmp-$NCC_{freeze\ dried}$ exhibited similar characteristic thermograms with similar peak melting temperatures, although Wmp-$NCC_{freeze\ dried}$ showed a slightly higher onset temperature which indicated higher crystallinity which predisposes them to resistance to thermal degradation due to stronger intermolecular bonds in their more ordered crystalline structure.[39] Therefore, the Wmp-native cellulose and Wmp-$NCC_{freeze\ dried}$ had the highest thermal stability among the cellulose samples. On the other hand, Wmp-$NCC_{oven\ dried}$ exhibited the lowest thermal stability. This may be due to the possible effect of the oven drying method employed which may have resulted in some degree of loss of its crystalline structure. This resulted in a lower onset temperature at 197°C as well as low peak melting temperatures at 200.67°C [Figure 4]. The thermal characteristics exhibited indicate weaker intermolecular bonds compared to Wmp-native cellulose and Wmp-$NCC_{freeze\ dried}$ which predisposes to less resistance in the packing and rearrangement of the particles which are the same factor that resulted in having a higher bulk and tapped density.[24]

The thermal stability demonstrated by Wmp-native cellulose and Wmp-$NCC_{freeze\ dried}$ allows for their ability to withstand the elevated temperatures involved in tablet manufacturing processes like granulation, drying, and compression without significant degradation or loss of functionality which is an important requirement for the structural stability and integrity of the tablet formulation.

TGA

The TGA thermogram [Figure 5] of the cellulose samples showed that they exhibited different thermal properties, but they followed a similar degradation pattern. All cellulose samples were stable at temperatures below 200°C; however, the Wmp-native cellulose and Wmp-$NCC_{freeze\ dried}$ were observed to have higher thermal stability than the Wmp-MCC and Wmp-$NCC_{oven\ dried}$ which corresponds with the observation in the DSC thermal analysis data, even though the temperature of onset of decomposition varied

when compared to those observed in the DSC analysis. At the end of the decomposition process, there was no trend in the weight of residue obtained at 694.9°C [Table 5] but Wmp-$NCC_{freeze\ dried}$ had the least residual weight at 14.89%.

The weight loss leading up to $T_{5\%}$ as the temperature of the sample increases corresponds to the evaporation of absorbed water.[40] The weight loss that occurred leading up to $T_{5\%}$ in the Wmp-$NCC_{freeze\ dried}$ (4.85%) and Wmp-$NCC_{oven\ dried}$ (5.66%) corresponds with the physicochemical characteristic that they exhibited in being redispersible in water because they contain residual moisture of about 4% by weight which is similar to the values observed on the TGA thermogram.[22] The redispersibility of Wmp-$NCC_{freeze\ dried}$ in water and the high thermal stability it exhibited shows that it has potential for use in tablet manufacturing processes involving high-temperature input such as hot melt extrusion where it would be resistant to degradation and when incorporated into a drug matrix could promote drug solubility and more efficient release of active pharmaceutical ingredient.

CONCLUSION

Watermelon peel residues have the potential to serve as a source of cellulose-based excipients for the low-cost production of pharmaceutical drug products. The watermelon peel residue-based cellulose biomaterials have the potential for application in tablet formulations and controlled drug delivery systems based on the reported physicochemical characteristics which can be explored in further studies. The acid hydrolysis treatment improved the physicochemical properties of the materials over native cellulose while the drying methods used affected the morphological and physicochemical characteristics of nanocrystalline cellulose. The freeze-dried nanocrystalline cellulose had better WHC, swelling capacity, smaller particle sizes, and a narrower PSD than the oven-dried sample.

Availability of data and material

The datasets generated and/or analyzed during the present study are not publicly available but are available from the corresponding author on reasonable request.

Authors' contributions

CPA and BAO conceived and designed the work. ARA and SJM carried out the experiments. ARA, CPA, BAO, and MO analyzed the data. The original manuscript was drafted by ARA while all the authors revised the manuscript. All authors read and approved the final manuscript.

Ethical approval

The Institutional Review Board approval is not required.

Declaration of patient consent

Patient's consent was not required as there are no patients in this study.

Financial support and sponsorship

None.

Conflicts of interest

There are no conflicts of interest.

Use of artificial intelligence (AI)-assisted technology for manuscript preparation

The authors confirm that there was no use of artificial intelligence (AI)-assisted technology for assisting in the writing or editing of the manuscript and no images were manipulated using AI.

REFERENCES

1. Sundarraj AA, Ranganathan TV. A review on cellulose and its utilization from agro-industrial waste. *Drug Invent Today.* 2018;10:89-94.
2. Seddiqi H, Oliaei E, Honarkar H, *et al*. Cellulose and its derivatives: Towards biomedical applications. *Cellulose*. 2021;28:1893-1931. doi: 10.1007/s10570-020-03674-w
3. Conte R. Cellulose recovery from waste. *IST J.* 2016, https://www.researchgate.net/profile/Raffaele-Conte/publication/316137803_Cellulose_recovery_from_waste
4. Petchsomrit A, McDermott MI, Chanroj S, *et al*. Watermelon seeds and peels: Fatty acid composition and cosmeceutical potential. *OCL*. 2020;27:3. doi:10.1051/ocl/2020051
5. Gin WA, Jimoh A, Abdulkareem AS, *et al*. Production of activated carbon from watermelon peel. *Int J Sci Eng Res*. 2014;5:66-71.
6. Zubairu A, Gimba A, Mamza W, *et al*. Proximate analysis of dry watermelon (*Citrullus lanatus*) rind and seed powder. *J Sci Eng Res*. 2018;5:473-478.
7. Latif A, Harun S, Sajab MS, *et al*. Ammonia-based pretreatment for ligno-cellulosic biomass conversion - an overview. *J Eng Sci Technol.* 2018;13:1595-1620.
8. Awoyale AA, Lokhat D. Experimental determination of the effects of pretreatment on selected Nigerian lignocellulosic biomass in bioethanol production. *Sci Rep.* 2021;11:557. doi: 10.1038/s41598-020-78105-8
9. Hindi S. Microcrystalline cellulose: The inexhaustible treasure for pharmaceutical industry. *Nanosci Nanotechnol Res*. 2017;4:17-24. doi: 10.12691/nnr-4-1-3
10. Aziz T, Ullah A, Fan H, *et al*. Nanocrystalline cellulose applications in health, medicine and catalysis. *J Polym Environ*. 2021;29:2062-2071. doi: 10.1007/s10924-021-02045-1
11. Akter F, Rifat SM, Rahman M, *et al*. Isolation of cellulosic material from drumstick pulp and outer shell of watermelon and preparation of their acetate and carboxymethyl derivatives.

Int J Adv Pharm Biol Chem. 2015;4(1):218-222.
12. AbdulKhalil HP, Sri Aprilia NA, Davoudpour Y, *et al*. Physicochemical characterisation of microcrystalline cellulose extracted from Kenaf bast. *BioResources*. 2016;11(2):3875-3889.
13. Sainorudin MH, Abdullah A, Rani MS, *et al*. Investigation of the structural, thermal and morphological properties of nanocellulose synthesised from pineapple leaves and sugarcane bagasse. *Curr Nanosci*. 2022;18:68-77. doi: 10.2174/1573413717666210216115609
14. Ohwoavworhua FO, Kunle OO, Ofoefule SI. Extraction and characterisation of microcrystalline cellulose derived from *Luffa* ellulosel plant. *Afr J Pharm Res Dev*. 2004;1:1-6.
15. Ordu JI, Udenze IE. Extraction and processing of pharmaceutical grade microcrystalline cellulose from *Dracaena arborea* stem. *J Sci Res Rep*. 2021;27:93-106. doi: 10.9734/jsrr/2021/v27i130352
16. Oyeniyi YJ, Achor M. The effect of drying techniques on the elastoplastic properties of locally processed microcrystalline cellulose. *Ife J Sci*. 2014;16:73-80.
17. Azubuike CP, Adeluola AO, Mgboko MS, *et al*. Physicochemical and microbiological evaluation of acidmodified native starch derived from *Borassus aethiopum* (*Arecaceae*) shoot. *Trop J Pharm Res*. 2018;17:883-890. doi: 10.4314/tjpr.v17i5.19
18. Oluwasina OO, Wahab O, Umunna Q, *et al*. *Dioscorea dumetorum* Pax as an alternative starch source for industrial applications. *J Appl Chem*. 2017;10:5-13. doi: 10.9790/5736-1005020513
19. Azubuike CP, Silva BO, Okhamafe AO. Pharmacopoeial and physicochemical properties of α-cellulose and microcrystalline cellulose powders derived from cornstalks. *Int J Green Pharm*. 2012;6:193-198. doi: 10.4103/0973-8258.104930
20. Makadia J, Seaton CC, Li M. Apigenin cocrystals: From computational prescreening to physicochemical property characterization. *Cryst Growth Des*. 2023;23:3480-3495. doi: 10.1021/acs.cgd.3c00030
21. British Pharmacopoeia Commission. Microcrystalline cellulose. In: British pharmacopoeia 2021. Vol. 1 and 2. United Kingdom: TSO (The Stationery Office); 2021.
22. Kumar A, Negi YS. Cellulose nanocrystals: Nanostrength for industrial and biomedical applications. In: Thakur VK, editor. Nanocellulose polymer nanocomposites. Massachusetts, CA: Scrivener Publishing LLC; 2015. p. 393-436.
23. Goudarzi M, Jouyban A, Soltanpour S. Influence of moisture content on the flow ability and compressibility of microcrystalline cellulose. *Powder Technol*. 2020;372:605-613.
24. Moravkar K, Korde S, Bhairav B, *et al*. Traditional and advanced flow characterisation techniques: A platform review for development of solid dosage form. *Indian J Pharm Sci*. 2020;82:945-957. doi: 10.36468/pharmaceutical-sciences.726
25. Krivokapić J, Ivanović J, Djuriš J, *et al*. Tableting properties of microcrystalline cellulose obtained from wheat straw measured with a single punch bench top tablet press. *Saudi Pharm J*. 2020;28:710-718. doi: 10.1016/j.jsps.2020.04.013
26. Mirhosseini H, Amid TB. Effect of different drying techniques on flow ability characteristics and chemical properties of natural carbohydrate-protein gum from Durian fruit seed. *Chem Cent J*. 2013;7:1-14. doi: 10.1186/1752-153X-7-1
27. Khazraji AC, Robert S. Interaction effects between cellulose and water in nanocrystalline and amorphous regions: A novel approach using molecular modeling. *J Nanomater*. 2013;2013:409676. doi: 10.1155/2013/409676
28. Álvarez-Castillo E, Bengoechea C, Felix M, *et al*. Freeze-drying versus heat-drying: Effect on protein-based superabsorbent material. *Processes*. 2021;9:1076. doi: 10.3390/pr9061076
29. Microtrac. Explanation of data reported by microtrac instruments; 2023. Available from: https://www.microtrac.com/files/3684/explanation-of-data-reported-by-microtrac-instruments.pdf# [Last accessed on 2023 Aug 08].
30. Sun Z, Ya N, Adams RC, *et al*. Particle size specifications for solid oral dosage forms: A regulatory perspective. American Pharmaceutical Review; 2010. Available from: https://www.americanpharmaceuticalreview.com/featured-articles/36779-particle-size-specifications-for-solid-oral-dosage-forms-a-regulatory-perspective [Last accessed on 2023 Dec 08].
31. Charoo NA. Critical excipient attributes relevant to solid dosage formulation manufacturing. *J Pharm Innov*. 2019;15:163-181. doi: 10.1007/s12247-019-09372-w
32. Kacurakova M, Capek P, Sasinkova V, *et al*. FT-IR study of plant cell wall model compounds: Pectic polysaccharides and hemicelluloses. *Carbohydr Polym*. 2020;43:195-203. doi: 10.1016/S0144-8617(00)00160-5
33. Agarwal UP, Reiner RS. Near-infrared spectroscopy and imaging of wood. In: Hernández RE, editor. Near-infrared Spectroscopy in Food Science and Technology. New York: John Wiley; 2016. p. 605-646.
34. Klemm D, Heublein B, Fink H, *et al*. Cellulose: Fascinating biopolymer and sustainable raw material. *Angew Chem Int Ed Engl*. 2005;44:3358-3393. doi: 10.1002/anie.200460587
35. Park S, Baker JO, Himmel ME, *et al*. Cellulose crystallinity index: Measurement techniques and their impact on interpreting cellulose performance. *Biotechnol Biofuels*. 2010;3:10. doi: 10.1186/1754-6834-3-10
36. Gong J, Li J, Xu J, *et al*. Research on cellulose nanocrystals produced from cellulose sources with various polymorphs. *RSC Adv*. 2017;7:33486-33493. doi: 10.1039/C7RA06222B
37. Johar N, Ahmad I, Dufresne A. Extraction, preparation and characterisation of cellulose fibres and nanocrystals from rice husk. *Ind Crops Prod*. 2012;37:93-99. doi: 10.1016/j.indcrop.2011.12.016
38. Haafiz M, Eichhorn SJ, Hassan A, *et al*. Isolation and characterisation of microcrystalline cellulose from oil palm biomass residue. *Carbohydr Polym*. 2013;93:628-634. doi: 10.1016/j.carbpol.2013.01.035
39. Yu Y, Wu D, Liu Y, *et al*. A review on cellulose-based functional materials derived from cellulose and cellulose derivatives. *Front Chem Sci Eng*. 2018;12:400-421.
40. Lu P, Hsieh Y. Preparation and properties of cellulose nanocrystals: Rods, spheres, and network. *Carbohydr Polym*. 2010;82:329-336. doi: 10.1016/j.carbpol.2010.04.073

How to cite this article: Azubuike CP, Adedokun AR, Oseni BA, *et al*. Characterization of physicochemical properties of microcrystalline and nanocrystalline cellulose powders derived from *Citrullus lanatus* peels for potential pharmaceutical applications. *Am J Pharmacother Pharm Sci* 2025:02.